



ARCHIVES
of
FOUNDRY ENGINEERING

DOI: 10.1515/afe-2017-0120

Published quarterly as the organ of the Foundry Commission of the Polish Academy of Sciences



ISSN (2299-2944)

Volume 17

Issue 3/2017

229 – 233

The Analysis of AISI A3 Type Ferritic-Austenitic Cast Steel Crystallization Mechanism

G. Stradomski

Czestochowa University of Technology, Faculty of Production Engineering and Materials Technology,
al. Armii Krajowej 19, 42-201 Czestochowa, Poland
Corresponding author. E-mail address: gstradomski@wip.pcz.pl

Received 12.04.2017; accepted in revised form 28.07.2017

Abstract

High-alloy corrosion-resistant ferritic-austenitic steels and cast steels are a group of high potential construction materials. This is evidenced by the development of new alloys both low alloy grades such as the ASTM 2101 series or high alloy like super or hyper duplex series 2507 or 2707 [1-5]. The potential of these materials is also presented by the increasing frequency of sintered components made both from duplex steel powders as well as mixtures of austenitic and ferritic steels [6, 7]. This article is a continuation of the problems presented in earlier works [5, 8, 9] and its inspiration were technological observed problems related to the production of duplex cast steel.

The analyzed AISI A3 type cast steel is widely used in both wet exhaust gas desulphurisation systems in coal fired power plants as well as in aggressive working environments. Technological problems such as hot cracking presented in works [5, 8], with are effects of the rich chemical composition and phenomena occurring during crystallization, must be known to the technologists.

The presented in this work phenomena which occur during the crystallization and cooling of ferritic-austenitic cast steel were investigated using numerical methods with use of the ThermoCalc and FactSage® software, as well with use of experimental thermal-derivative analysis.

Keywords: Duplex cast steel, Solidification, Numerical methods, DTA, Peritectic reaction, Sigma phase.

1. Introduction

Despite the growing interest in alternative energy sources, which is related both with environmental regulations and growing public awareness, fossil fuels including oil and natural gas will continue to be a huge market for high alloy steel products for many years to come.

Materials, which for more than 40 years, regardless of the periods of prosperity or crises exhibited constant, about 5% annual increase in production, are steels and corrosion resistant steels. Very diversified properties, depending on the chemical

composition and microstructure, are constantly expanding the applications of these materials. A particular group are ferritic-austenitic steels, whose development allows for increased permanence of elements working under erosion and corrosion condition or the exploitation of heavily burdened, strongly sulfated gas and oil deposits.

Thanks to high strength and plastic properties [10-14], they can be used on mining platforms and in deep wells, even at a depth of 8000 meters, where the pressure can reaches 1600 bar and the temperature is 300°C. Geological data of Poland indicate [15] that our country has a large geothermal energy potential and is a site for industrial wells. Taking industrial extraction requires a

large number of deep shaft, up to 3000 meters, due to the nature of the deposits, materials that are dedicated to these operating conditions are corrosion resistant steels, especially ferritic-austenitic steels.

2. Research material and methodology

The subject of research was the AISI grade A3 cast steel with the addition of about 2.5% copper, the chemical composition is presented in Table 1. The steel was melted in industrial conditions by one of the indigenous producers during technological trials. Presented results include the analysis of the crystallization mechanism using numerical tools with use of FactSage® and ThermoCalc applications, and experimental thermal-derivative analysis (DTA), in addition the results of microstructure analysis performed with use of the Nikon Ma 200 optical microscopes and SEM were made. The numerical analysis was made for the equilibrium state, the temperature of the simulation beginning was taken 1600°C. The melting temperature during DTA test was lower (about 1530°C), what was dictated by the furnace parameter.

In this work will be also prove that the test alloy appear the peritectic reaction which also has an effect on the final properties.

Table 1.

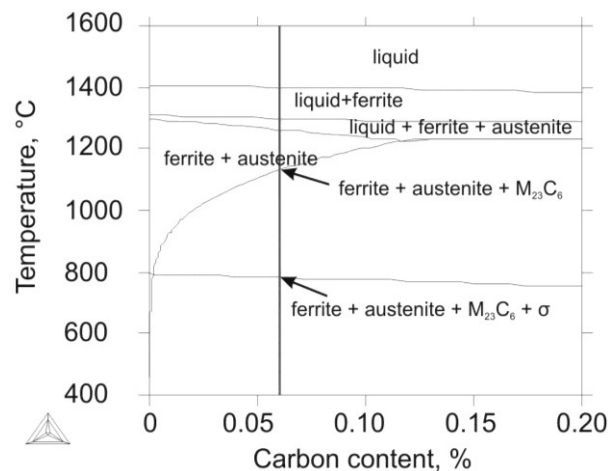
Chemical composition of the examined cast steel wt.%

No.	C	Cr	Ni	Cu	Mo	Mn	Si	S
Cast	0.0613	23.38	8.58	2.41	2.94	0.063	1.07	0.0331
	P	N	S	Co	Al<	V	W	
	0.0262	0.064	0.0331	0.122	0.001	0.0723	0.0911	

2. Research results and their discussion

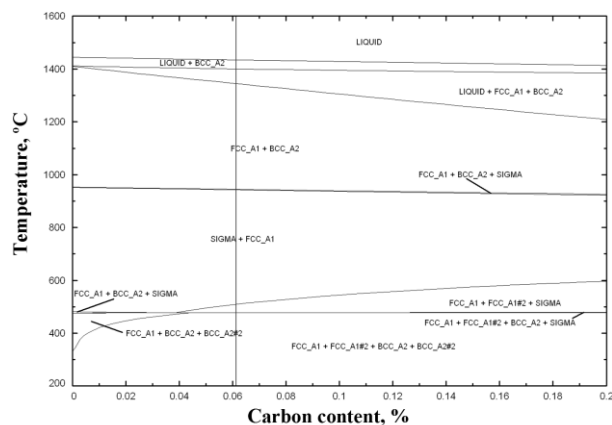
The phenomena occurring during the solidification and cooling of ferritic-austenitic cast steels was determined on the basis of numerical analysis for equilibrium state are presented in Figures 1 and 2.

Crystallization of the alloy, whose chemical composition is marked by vertical lines, starts at about 1404°C, according to the ThermoCalc or 1436°C according to FactSage® and is associated with the precipitation of ferrite. Below this temperature, begin the peritectic transformation, which in multi-component systems do not appear at constant temperature and hence to this the coexistence of three phases: liquid, ferrite, austenite is present. According to ThermoCalc's a peritectic reaction takes place, in the range of temperature 1301-1264°C, while according to FactSage® it extends to about 1345°C. Transformation of the part of ferrite into austenite depend on the applied tool begin at 1345°C or 1264°C. It is the transformation of ferrite into austenite, which determines the exceptional, distinctive properties of duplex cast steels. ThermoCalc, in contrast to FactSage®, showed that below 1131°C the Cr₂₃C₆ carbide precipitation appears. At about 936°C (FactSage®) or 783°C (ThermoCalc), for the analyzed chemical composition, the intermetallic σ phase precipitation begins and about 567°C or 510°C finish.



Temperature	Phase content
above 1404°C	liquid
1404°C - 1301°C	liquid + ferrite
1301°C - 1264°C	liquid + ferrite + austenite
1264°C - 1131°C	ferrite + austenite
1131°C - 783°C	ferrite + austenite + M ₂₃ C ₆
783°C - 567°C	ferrite + austenite + M ₂₃ C ₆ + σ phase
below 567	ferrite + austenite + M ₂₃ C ₆ + σ phase

Fig. 1. Results of numerical analysis obtained with use of ThermoCalc software



Temperature	Phase content
1345°C - 936°C	ferrite + austenite
936°C - 510°C	ferrite + austenite + σ phase
below 510	ferrite + austenite + σ phase

Fig. 2. Results of numerical analysis obtained with use of FactSage® software

The divergence obtained from numerical data required verification. For this purpose, a thermal-derivative analysis (DTA) was made. From the material under the cover of argon in an induction furnace, a very fast (90s) melt at about 1530°C of 350g alloy was made. Such experimental conditions ensured the

consistency of the chemical composition, which was confirmed by the spectral analysis of materials before and after the melting. Obtained result was presented on Figure 3.

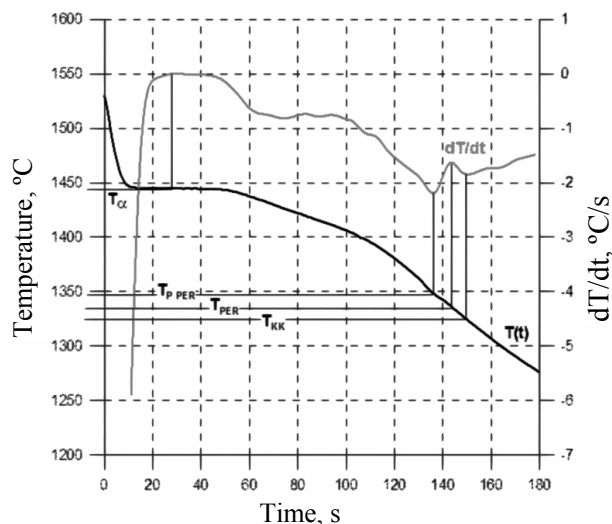


Fig. 3. The DTA scheme with marked characteristic points

While the begin of crystallization based on Experimental (DTA) and Numerical Data from the FactSage® show a high convergence - 9°C, however its range is 60°C variant.

Satisfactory convergence of 20°C of the reaction temperature was found for results obtained in FactSage® and DTA. The values obtained in ThermoCalc present significant differences, indicating that the numerical calculations based on thermodynamic values for such complex compound compositions should be to be considered only as indicative for the crystallization and transition processes.

Table 2 present comparison of obtained numerical and experimental data.

In addition, the analysis of the microstructure of the DTA specimen was made in order to verify the obtained results. Microstructure analysis etched with the Mi21Fe reagent (30g potassium ferricyanide, 30g potassium hydroxide and 60g distilled water) was made with use of Nikon Eclipse MA-200 microscope. The results of the microstructural studies are presented in Figures 4 and 6. Figure 4 shows an area of about 4.5x3.5 mm with a magnification of 50x allowing making overall analysis.

Table 2.

Characteristic temperatures of the test alloy determined with use of various tools

Tool	Crystallization progress									
	Liquid + ferrite		Liquid + ferrite + austenite		Ferrite + austenite		Ferrite + austenite + $M_{23}C_6$		Sigma	
	Temperature, °C		Temperature °C		Temperature, °C		Temperature, °C		Temperature, °C	
	Begin	End	Begin	End	Begin	End	Begin	End	Begin	End
FactSage®	1436	1400	1400	1345	1345	936	-	-	936	510
ThermoCalc	1404	1301	1301	1264	1264	1131	1131	783	783	567
DTA	1445	1349	1349	1325	-	-	-	-	918	647

* liquid + ferrite + austenite + $M_{23}C_6$

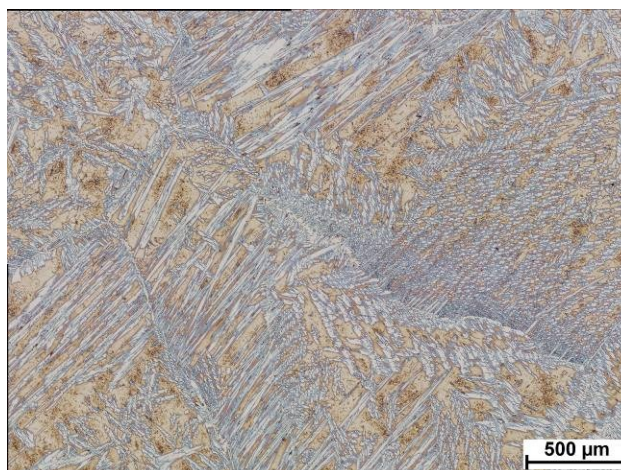


Fig. 4. Microstructure of the test alloy with visible dendrites of liquid of the crystallization end 50x

Dendritic austenite precipitation within a wide angular grains particularly visible in Figure 4 confirm the occurrence of peritectic reaction in the final stage of crystallization.

The scheme of peritectic reaction mechanism for the tested cast steel, drawn on the base of reference [15] is shown in Figure 5.

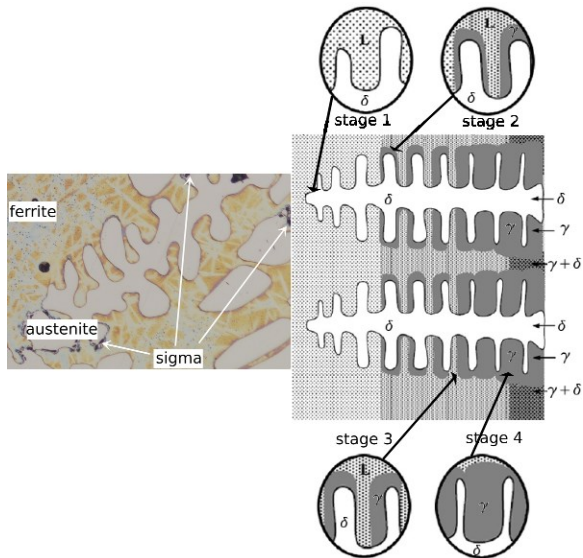


Fig. 5. Scheme of growth of the primary and peritectic during peritectic crystallization and examples of the dendritic structure of the end of crystallization disclosed in the DTA sample

Authors of the paper [16] have distinguished four stages of dendritic crystallization, including their degree of advanced. For peritectic alloys with initial chemical composition C_0 crystallization can take place according to peritectic and eutectic reactions. In the stage 1 are present only liquid and δ phase, in the stage 2 begin precipitation of the γ phase on the border of δ . Next in stage 3 from the liquid in border area δ - γ increase the amount of the γ at the cost of δ . Stage 4 the amount of liquid is very low and the amount of γ increase at the cost of the δ phase till the liquid exist.

Beside to the presence of columnar and equatorial crystals (Figure 4) typical of castings, the presence of phase σ (Fig. 6) was found in the central part of the probe near the thermocouple location. The positioning of the thermocouple in this part of the sample allowed very precise determination of the time and the cooling rate. The cooling time in the temperature range of 1050-550°C was about 12 minutes and the speed was about 42°C/min. It have to be marked that the particular intensity of phase precipitations σ were observed near the liquid of the end crystallization dendritic structures.

The presence of phase σ in the tested alloy described by the author in more detail in publication [5] was also recorded during the DTA analysis (Fig. 6). This is interesting because the method is not so sensitive. However, the specific location of precipitations near crystals of the liquid of the end of crystallization, very close to the thermocouple, most likely allowed to record the temperature range of its secretion.

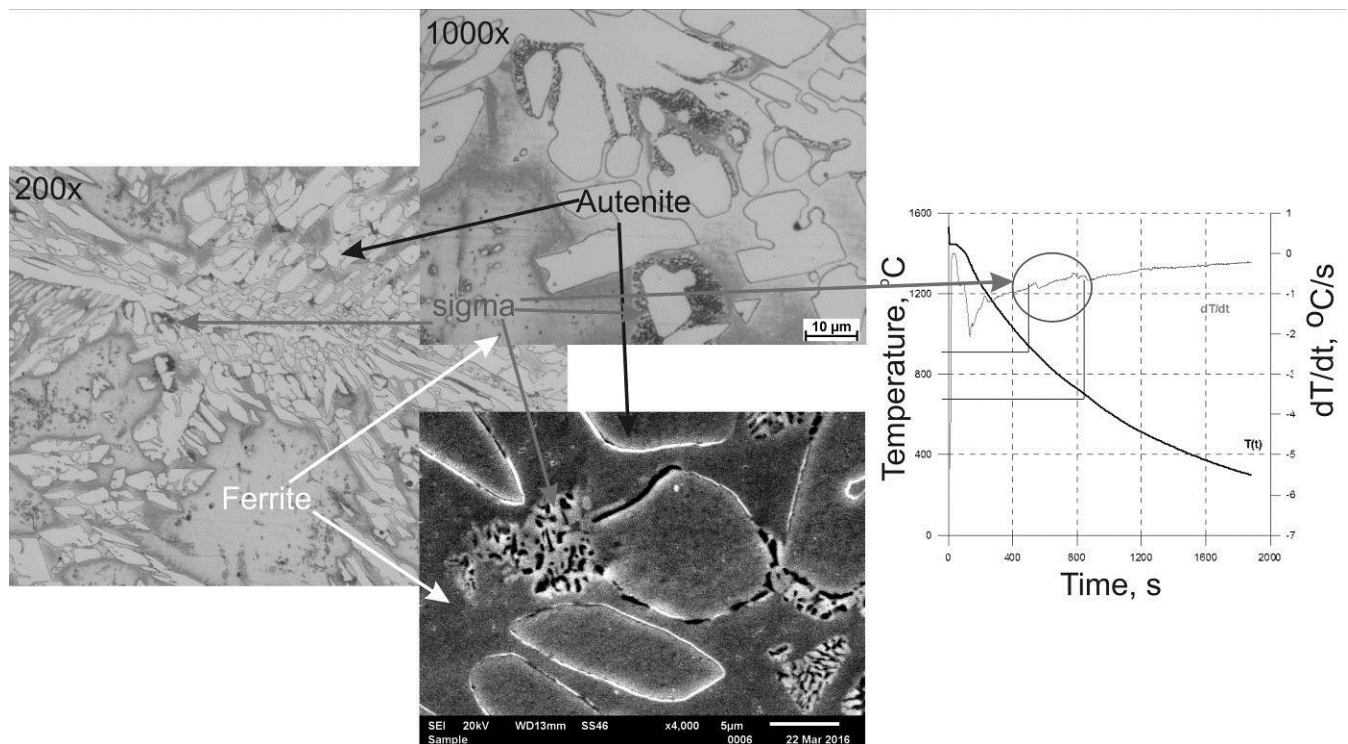


Fig. 6. The microstructure of the test alloy together with the identified phases, and the ATD plot for the entire test range

4. Summary

The cast steel crystallize as ferritic, what was confirmed by the equilibrium state numerical analysis results made with use of FactSage® and ThermoCalc application. The theoretical analysis indicates the possibility of occurring of the peritectic reaction in the final phase the crystallization. Because of the incompatibility in the obtained numerical data (Table 2), the most reliable results are, however, the results of the thermal-derivative (DTA) analysis.

Analysis of the microstructure of both the overall view (Fig. 4) and much more accurately (Fig. 6) confirmed the results of numerical and experimental investigations of the crystallization process. Presented on the Figure 5 developed on the basis of the work [14] scheme of growth of the primary and peritectic phases during peritectic crystallization was also reflected in material's structure.

Cooling time of about 12 minutes in the temperature range of 1050-550°C, and a speed of about 42°/min was sufficient for σ phase precipitations to occur. This phase precipitates at the boundary of the liquid of the end of crystallization dendrites in the area where the peritectic reaction occurs. What is interesting the temperature range of its secretion, was also recorded during DTA analysis.

References

- [1] Shargay, C. (2005). Application of duplex stainless steels in refining. *Stainless Steel World*. 17, 19-27.
- [2] Marken, L. (2005). Application of duplex and super duplex stainless steels in the offshore industry- Case histories. *Stainless Steel World Conference & Expo*, Maastricht, Netherlands 8-10 November, p. 318-323.
- [3] Practical Guidelines for Fabrication of Duplex Stainless Steels. International Molybdenum Association, (2009).
- [4] Kalandyk, B. & Wojtal, W. (2013). Effects of steel - applied for large-dimension castings for the power engineering - refining in the ladle-furnace. *Archives Of Metallurgy And Materials*. 58(3), 779-783.
- [5] Stradomski, G. (2016). *Effect of sigma phase morphology on the properties of steel and duplex steels*. Częstochowa. ISBN 978-83-63989-44-6, ISSN 2391-632X. (in Polish).
- [6] Dudek, A., Wronska, A. & Adamczyk, L. (2014). Surface remelting of 316 L+434 L sintered steel: microstructure and corrosion resistance. *Journal of Solid State Electrochemistry*. 18(11), 2973-2981.
- [7] Busschaert, F., Élodie, J. (2014). Oil and Gas end-user experience on HIPped components, 11th International Conference of Hot Isostatic Pressing, HIP '14, p.1-14.
- [8] Stradomski, G. (2016). The Cracking Mechanism of Ferritic-Austenitic Cast Steel. *Archives of Foundry Engineering*. 16(4), 153-156. ISSN 1897-3310, 2299-2944.
- [9] Stradomski, G. (2015). *The X2CrNiMo25-6-3 Duplex Steel Plasticity - Complementation*, Ostrava: TANGER Ltd., METAL 2015. 24th International Conference on Metallurgy and Materials. June 3rd - 5th 2015, Brno, Czech Republic.
- [10] Dyja, D., Stradomski, Z., Kolan, C., Stradomski, G. (2012). Eutectoid decomposition of δ -ferrite in ferritic-austenitic duplex cast steel – structural and morphological study. *Thermec. Materials Science Forum Vols. 706-709*, p. 2314–2319
- [11] Voronenko, B.I. (1997). Austenitic-ferritic stainless steels: A state-of-the-art review. *Metal Science and Heat Treatment*. 39(10), 428-437.
- [12] Stradomski, G. (2014). *The Assessment of the X2CrNiMo25-6-3 Duplex Steel Plasticity*. Ostrava: TANGER Ltd., METAL 2014. Conference METAL 2014 Proceedings. 23rd International Conference on Metallurgy and Materials. May 21st - 23rd, Brno, Czech Republic.
- [13] Chih-Chun, H., Dong-Yih, L. & Weite, W. (2007) Precipitation behavior of σ phase in 19Cr-9Ni-2Mn and 18Cr-0.75Si stainless steels hot-rolled at 800 °C with various reduction ratios. *Materials Science and Engineering A*. 467(1-2), 181-189.
- [14] Giętka, T., Ciechacki, K. & Kik, T. (2016). Numerical Simulation of Duplex Steel Multipass Welding. *Archives of Metallurgy and Materials*. 61(4), 1975 - 1984.
- [15] Górecki, W. (red.) i in. (2011). *Atlas of water resources and geothermal energy of the Western Carpathians*. Kraków: AGH KSE. (in Polish).
- [16] Dongmei, L., Xinzhong, L., Yanqing, S., Peng, P., Liangshun, L., Jingjie, G. & Hengzhi, F. (2012). Secondary dendrite arm migration caused by temperature gradient zone melting during peritectic solidification. *Acta Materialia*. 60, I. 6-7, 2679-2688.